Microelectronic Engineering 87 (2010) 2482–2487

Contents lists available at ScienceDirect

Microelectronic Engineering

journal homepage: www.elsevier.com/locate/mee

Electrical analysis of organic dye-based MIS Schottky contacts

Ö. Güllü [a,*], A. Türüt [b]

[a] Batman University, Faculty of Sciences and Arts, Department of Physics, Batman, Turkey
[b] Atatürk University, Faculty of Science, Department of Physics, Erzurum, Turkey

ARTICLE INFO

Article history:
Received 31 October 2009
Received in revised form 15 April 2010
Accepted 16 May 2010
Available online 27 May 2010

Keywords:
Schottky diode
Interface states
Series resistance
Organic thin film

ABSTRACT

In this work, we prepared metal/interlayer/semiconductor (MIS) diodes by coating of an organic film on *p*-Si substrate. Metal(Al)/interlayer(Orange G=OG)/semiconductor(*p*-Si) MIS structure had a good rectifying behavior. By using the forward-bias *I–V* characteristics, the values of ideality factor (*n*) and barrier height (BH) for the Al/OG/*p*-Si MIS diode were obtained as 1.73 and 0.77 eV, respectively. It was seen that the BH value of 0.77 eV calculated for the Al/OG/*p*-Si MIS diode was significantly larger than the value of 0.50 eV of conventional Al/*p*-Si Schottky diodes. Modification of the potential barrier of Al/*p*-Si diode was achieved by using thin interlayer of the OG organic material. This was attributed to the fact that the OG organic interlayer increased the effective barrier height by influencing the space charge region of Si. The interface-state density of the MIS diode was found to vary from 2.79×10^{13} to 5.80×10^{12} eV^{-1} cm^{-2}.

1. Introduction

In recent years, there has been growing interest in the field of thin organic semiconducting films due to their successful application in optical and electronic devices [1–6]. In addition, organic materials have now reached the early stages of commercialization with the technological success of thin film organic optoelectronic devices, particularly organic light-emitting devices and with improving their efficiency, manufacturing yield and long-term stability [1–6]. Owing to their stability and barrier height (BH) enhancement properties, organic materials have been employed particularly in electronic devices [7–10]. Forrest et al. [8,11] and Antohe et al. [12] obtained metal–interfacial layer–semiconductor (MIS) contacts by sublimation of organic thin films on a semiconductor substrate, subsequently evaporation of different metals and then measured their ideality factors and BHs. Aydin et al. [10] obtained MIS contacts by addition of a β-carotene solution on top of the Si substrate and waited for evaporation of the solution and then measured the ideality factor and the BH. Kilicoglu et al. [7] obtained MIS contacts by addition of a methyl red solution on top of the Si substrate and waited for evaporation of the solution, and then measured the ideality factor and the BH. They [7–13] showed that these contacts for organic thin films formed at metal/semiconductor structures had rectification and enhancement of BH properties.

The electrical properties of metal/semiconductor (MS) structures can be modified by organic semiconductors when an organic layer is inserted between the inorganic semiconductor and metal. The studies made in literature have shown that the barrier height could be either increased or decreased by using organic thin layer on inorganic semiconductor [5–13]. The new electrical properties of the MS contacts can be promoted by means of the choice of suitable organic semiconductor [5]. Orange G (OG) has also attracted the researchers' attentions due to their easiness of synthesis, good environmental stability and high degree humidity response, but unfortunately a little amount of information is available in scientific literature about electrical properties of OG [14]. OG with molecular formula $C_{16}H_{10}N_2O_7S_2Na_2$ (1,3-naphthalenedisulfonic acid, 7-hydroxy-8-(phenylazo)-, disodium salt) used in this study is a typical aromatic azo compound. The molecular structure of the OG is given in Fig. 1. Recently, the structure of organic dyes has attracted considerable attention due to their wide applicability in the light-induced photo isomerization process, and their potential usage for the reversible optical data storage [15]. OG organic material has been considered as one of the most stable organic semiconductors for various electronic and optoelectronic applications and has not previously been used for the fabrication of different electronic devices. Our aim is to investigate the electrical properties of Al/OG/*p*-Si diode by the insertion of OG organic layer between Si semiconductor and Al metal by using current–voltage (*I–V*) and capacitance–voltage (*C–V*) measurements and is to compare the electrical parameters of the Al/OG/*p*-Si MIS diode with those of conventional MS diodes. Also, optical absorbance spectrum of the OG organic film on a glass substrate will be analyzed in the UV–vis region.

* Corresponding author. Tel.: +90 488 217 3620; fax: +90 488 215 7201.
E-mail address: omergullu@gmail.com (Ö. Güllü).

0167-9317/$ - see front matter © 2010 Elsevier B.V. All rights reserved.
doi:10.1016/j.mee.2010.05.004

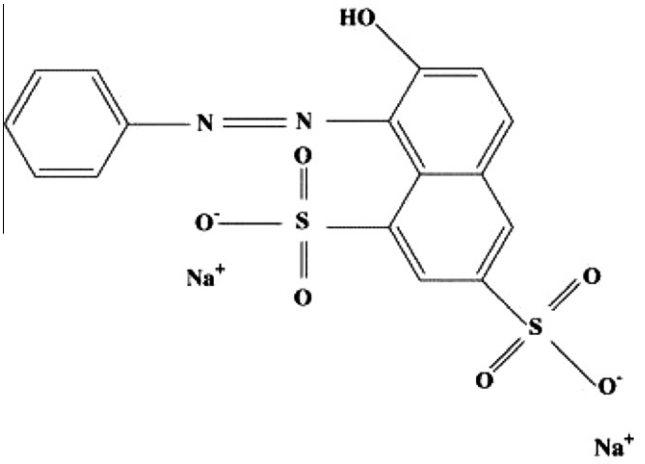

Fig. 1. The molecular structure of OG molecule.

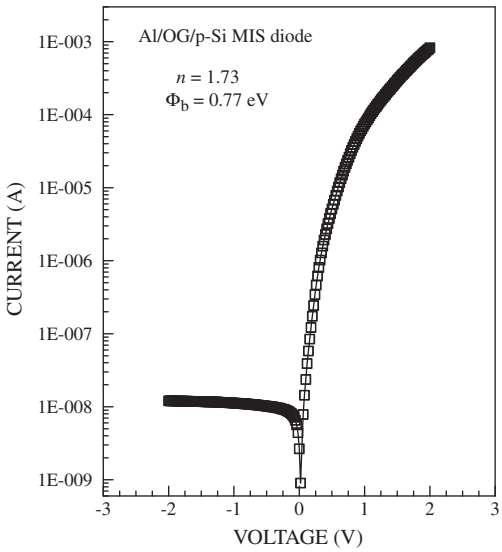

Fig. 3. Current–voltage characteristic of the Al/OG/*p*-Si MIS diode.

2. Experimental details

Al/OG/*p*-Si MIS diodes were prepared by using one side polished (as received from the manufacturer) *p*-type Si wafer with (1 0 0) orientation and 4.94×10^{14} cm^{-3} doping density obtained from *C–V* measurements in this study. The wafer was chemically cleaned by using the RCA cleaning procedure (i.e., a 10 min boil in $NH_3 + H_2O_2 + 6H_2O$ followed by a 10 min boil in $HCl + H_2O_2 + 6H_2O$). The native oxide on the front surface of Si substrate was removed by using HF:H_2O (1:10) solution and then it was rinsed in de-ionized water for 30 min. Then, low resistivity ohmic contact on *p*-type Si substrate was made by using Al metal, followed by a temperature treatment at 570 °C for 3 min in N_2 atmosphere. After cleaning procedures and ohmic contact metallization were carried out, OG organic film was directly formed by adding 6 μL of the OG solution (wt 0.2% in ethanol) on the front surface of the *p*-Si wafer, and evaporated by itself for drying of solvent in N_2 atmosphere for 30 min. The contacting metal dots were formed by evaporation of Al metal with diameter of 1.0 mm (diode area = 7.85×10^{-3} cm^2). All evaporation processes were carried out in a vacuum coating unit at about 10^{-5} mbar. *I–V* and *C–V* measurements for Al/OG/*p*-Si MIS diode were measured by using a Keithley 487 Picoammeter/Voltage source and a HP 4192A LF Impedance Analyzer, respectively, at room temperature and in dark conditions (see Fig. 2). Also, optical absorbance spectrum of the OG thin film on a glass substrate was taken with a spectrophotometer (LKB Biochrom Ultraspec II).

3. Results and discussion

3.1. Analysis of current–voltage characteristic of the Al/OG/p-Si MIS structure

Fig. 3 shows the experimental semi-log *I–V* characteristic of the Al/OG/*p*-Si MIS Schottky device at room temperature. As clearly seen from Fig. 3, the Al/OG/*p*-Si Schottky structure is rectifying. The weak voltage dependence of the reverse-bias current and the exponential increase of the forward-bias current are the characteristic properties of rectifying contacts. The current curve in forward-bias region becomes dominated by series resistance from contact wires or bulk resistance of the organic semiconductor and the inorganic semiconductor giving rise to the curvature at high current in the semi-log *I–V* plot. By using thermionic emission (TE) theory [16,17], the ideality factor (n) and BH (Φ_b) can be obtained from the slope and the current axis intercept of the linear region of the forward-bias *I–V* plot, respectively. The values of the BH and the ideality factor for the Al/OG/*p*-Si diode have been calculated as 0.77 eV and 1.73, respectively. The ideality factor determined by the image-force effect alone should be close to 1.01 or 1.02 [18–20]. Higher values of ideality factors are attributed to secondary mechanisms which include interface dipoles due to interface doping or specific interface structure as well as fabrication-induced defects at the interface [18–21]. According to Tung [20], the large values of n may also be attributed to the presence of a wide distribution of low-Schottky barrier patches caused by laterally barrier inhomogeneous. Also, the image-force effect, recombination–generation, and tunneling may be possible mechanisms that could lead to an ideality factor value greater than unity [16].

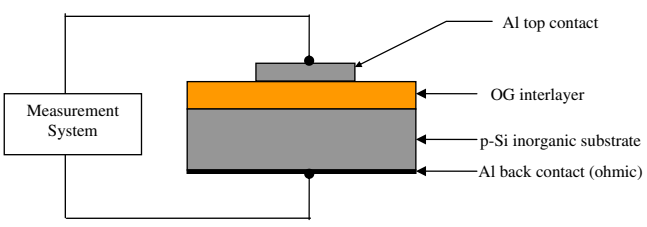

Fig. 2. The schematic structure of the Al/OG/*p*-Si MIS device.

The BH value of 0.77 eV that we have obtained for the Al/OG/*p*-Si device due to OG organic layer is remarkably higher than that achieved with conventional MS contacts such as Al/*p*-Si diode, whose BH was 0.50 eV [22]. In literature, some experimental studies have been reported for the barrier height modification by using the organic thin films [23]. Recently, Temirci and Çakar [24] have published a paper about Cu/Rhodamine-101/*p*-Si/Al diode with barrier height value of 0.78 eV and ideality factor value of 1.54. The obtained barrier height value of the diode was higher than the conventional Cu/*p*-Si [17]. In other study, Karatas et al. [25] have fabricated an Al/Rh101/*p*-Si/Al contact. The barrier height (0.817 eV) of the Al/Rh101/*p*-Si/Al contact was significantly larger than the barrier height of conventional Al/*p*-Si Schottky diode. In another study, Çakar et al. [26] have fabricated the Cu/pyronine-B/*p*-Si, Au/pyronine-B/*p*-Si, Al/pyronine-B/*p*-Si and Sn/pyronine-B/*p*-Si diodes, and the obtained barrier heights for these diodes were larger than the conventional metal/*p*-Si contact. They [26] have evaluated that the barrier height could be enhanced or modified by using thin interfacial films. It is seen from the above results that the organic layer can be used to vary the effective barrier height of

Al/*p*-Si Schottky diodes. Furthermore, this case may be ascribed to the organic interlayer modifying the effective barrier height by influencing the space charge region of the inorganic substrate [27–30]. The OG organic layer forms a physical barrier between the Al metal and the *p*-Si wafer. This organic layer can produce substantial shift in the work function of the metal and in the electron affinity of the semiconductor and in turn, the organic layer gives an excess barrier of 0.27 eV, i.e., the OG organic layer increases the barrier height of Al/*p*-Si. The barrier height of Al/*p*-Si contact increases by the insertion of a dipole layer between *p*-Si semiconductor and OG organic layer. Similarly, Zahn et al. [31] have indicated that the initial increase or decrease in effective barrier height for the organic interlayer was correlated with the energy level alignment of the lowest unoccupied molecular orbital with respect to the conduction band minimum of the inorganic semiconductor at the organic/inorganic semiconductor interface. The obtained results and previous studies have shown that the electrical conductivity, preparation process of organic film, film thickness of the organic semiconductor to be used in device fabrication significantly affect the device performance and electronic parameters of the MS devices. As a result, we have evaluated that Al/*p*-Si MS diode could be designed to exhibit the desired properties by means of the choice of the organic molecule [23].

It is well known that the downward concave curvature of the forward-bias current–voltage plots at sufficiently large voltages is caused by the effect of series resistance (R_s), apart from the interface states, which are in equilibrium with the semiconductor [32]. The R_s values have been calculated by using a method developed by Cheung and Cheung [33,34]. According to Cheung and Cheung [34], the forward-bias *I–V* relation of a Schottky diode with the series resistance can be expressed as:

$$I = I_0 \exp\left[\frac{q(V - IR_s)}{nkT}\right], \tag{1}$$

where IR_s term is the voltage drop across series resistance of device. The values of the series resistance can be determined from following functions by using Eq. (1):

$$\frac{dV}{d(\ln I)} = \frac{nkT}{q} + IR_s, \tag{2}$$

$$H(I) = V - \left(\frac{nkT}{q}\right)\ln\left(\frac{I}{AA^*T^2}\right), \tag{3}$$

and $H(I)$ is given as follows:

$$H(I) = n\Phi_b + IR_s, \tag{4}$$

A plot of $\frac{dV}{d(\ln I)}$ vs. I will be linear and gives R_s as the slope and $\frac{nkT}{q}$ as the *y*-axis intercept from Eq. (2). Fig. 4 shows a plot of $\frac{dV}{d(\ln I)}$ vs. I at room temperature. The values of n and R_s have been calculated as $n = 6.61$ and $R_S = 634.2\ \Omega$, respectively. It is observed that there is a large difference between the value of n obtained from the forward-bias ln*I–V* plot and that obtained from the $dV/d(lnI) - I$ curve (see Fig. 4). This may be attributed to the existence of the series resistance and interface states and to the voltage drop across the interfacial layer (native oxide plus OG organic layer) [35].

Besides, $H(I)$ vs. I plot have to be linear according to the Ref. [34]. The slope of this plot gives a different determination of R_s. By using the value of n obtained from Eq. (2), the value of Φ_b is obtained from the *y*-axis intercept. $H(I)$ vs. I curve is shown in Fig. 4. From $H(I)$ vs. I plot, Φ_b and R_s have been calculated as 0.66 eV and 825.3 Ω, respectively.

Norde proposed an alternative method to determine value of the series resistance [36]. The following function has been defined in the modified Norde's method:

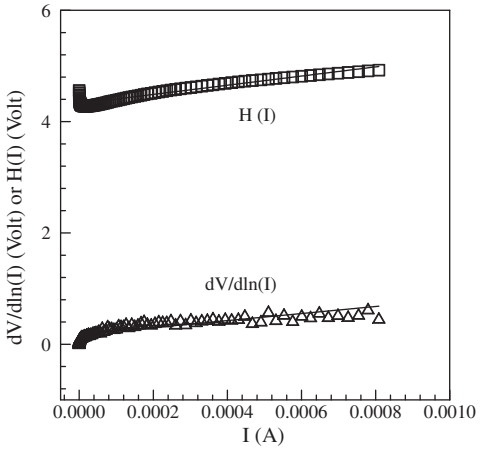

Fig. 4. $dV/d\ln I$–I and $H(I)$–I plots obtained from the experimental *I–V* data in Fig. 3.

$$F(V) = \frac{V}{\gamma} - \frac{1}{\beta}\ln\left(\frac{I(V)}{AA^*T^2}\right) \tag{5}$$

where γ is an integer (dimensionless) greater than n. $I(V)$ is current obtained from the *I–V* curve and β is a temperature-dependent value calculated with $\beta = q/kT$. Once the minimum of the F vs. V plot is determined, the value of barrier height can be obtained from Eq. (6),

$$\Phi_b = F(V_0) + \frac{V_0}{\gamma} - \frac{kT}{q} \tag{6}$$

where $F(V_0)$ is the minimum point of $F(V)$ and V_0 is the corresponding voltage.

Fig. 5 shows the $F(V)$–V plot of the junction. From Norde's functions, R_s value can be determined as:

$$R_s = \frac{kT(\gamma - n)}{qI}. \tag{7}$$

From the *F–V* plot by using $F(V_0) = 0.76$ V and $V_0 = 0.14$ V values, the values of Φ_b and R_s of the Al/OG/*p*-Si structure have been determined as 0.80 eV and $1.20 \times 10^5\ \Omega$, respectively. There is a difference in the values of Φ_b obtained from the forward-bias ln*I–V*, Cheung functions and Norde functions. Differences in the barrier height values obtained from three methods for the device may be attributed to the extraction from different regions of the forward-bias current–voltage plot [37]. However, the value of series resistance obtained from Norde function is higher than that ob-

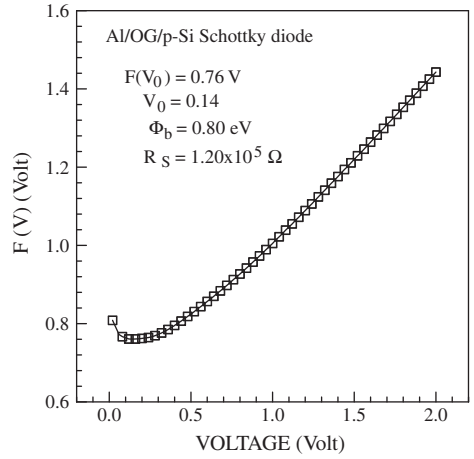

Fig. 5. $F(V)$–V plots obtained from the experimental *I–V* data in Fig. 3.

tained from Cheung functions. Cheung functions are only applied to the nonlinear region in high voltage section of the forward-bias ln*I*–*V* characteristics, while Norde's functions are applied to the full forward-bias region of the ln*I*–*V* characteristics of the junctions [37]. The value of series resistance may also be large for the higher ideality factor values. Furthermore, the value of series resistance is very high for this device. This indicates that the series resistance is a current-limiting factor for this structure. The effect of the series resistance is usually modeled with series combination of a diode and a resistance R_s. The voltage drop across a diode is expressed in terms of the total voltage drop across the diode and the resistance R_s. The very high series resistance behavior may be ascribed to decrease of the exponentially increasing rate in current due to space charge injection into the OG organic thin film at higher forward-bias voltage [37]. Furthermore, Norde's model may not be a suitable method especially for the high ideality factor of the rectifying junctions, which are non-agree with pure thermionic emission theory. Therefore, the series resistance value from Norde functions can be much higher than one from Cheung model for especially non-ideal rectifying structures [37].

3.2. Analysis of interfacial properties of the Al/OG/p-Si MIS structure

For a metal/semiconductor diode having interface states in equilibrium with the semiconductor the ideality factor n becomes greater than unity as proposed by Card and Rhoderick [38] and then interface-state density N_{SS} is given by:

$$N_{SS} = \frac{1}{q}\left[\frac{\varepsilon_i}{\delta}(n(V)-1) - \frac{\varepsilon_s}{w}\right] \tag{8}$$

where w is the space charge width, ε_s is the permittivity of the semiconductor, ε_i is the permittivity of the interfacial layer, δ is the thickness of organic layer, and $n(V) = \frac{V}{(kT/q)\ \ln(I/I_0)}$ is voltage dependent ideality factor. In p-type semiconductors, the energy of the interface states E_{SS} with respect to the top of the valence band at the surface of the semiconductor is given by:

$$E_{SS} - E_V = q\Phi_b - qV \tag{9}$$

where V is the voltage drop across the depletion layer and Φ_b is the effective barrier height. The energy distribution or density distribution curves of the interface states can be determined from experimental data of this region of the forward-bias I–V plot. Substituting the voltage dependent values of n and the other parameters in Eq. (8), the N_{SS} vs. E_{SS}–E_V plot was obtained as shown in Fig. 6. It is seen that N_{SS} value decreases with increasing E_{SS}–E_V value. The density distribution of the interface states of the diode changes from 2.79×10^{13} to 5.80×10^{12} eV^{-1} cm^{-2}. Aydogan et al. [32] found that the deposition of polymers onto the inorganic semiconductor could generate large number of interface states at the semiconductor surface, which strongly influence the properties of the PANI/p-Si/Al structure. Çakar et al. [39] have determined interface properties of Au/PYR-B/p-Si/Al contact. They [38] have found that the interface-state density values varied from 4.21×10^{13} to 3.82×10^{13} cm^{-2} eV^{-1}. In another study, Aydin and Türüt [40] have investigated the interface-state density properties of the Sn/methyl-red/p-Si/Al diode and interface-state density was found to vary from 1.68×10^{12} to 1.80×10^{12} cm^{-2} eV^{-1}. The interface-state density of the Al/OG/p-Si diode is consistent with those of above mentioned diodes. It is evaluated that interface properties of Al/p-Si junction are changed by depending on organic layer inserted into metal and semiconductor. The organic interlayer appears to cause to a significant modification of interface states even though the organic–inorganic interface appears abrupt and unreactive [41–43]. The OG organic layer increases the effective barrier height clearly upon the modification of the semiconductor surfaces and the chemical interaction at the interface of the OG organic layer to the p-Si and oxide–organic interface states will give rise to new interface states [23].

3.3. Analysis of capacitance–voltage characteristic of Al/OG/p-Si MIS diode

For MIS diodes, the capacitance–voltage measurements can provide knowledge about the fixed charge concentration and barrier height. Any variation of the charge within a p–n diode with an applied voltage variation yields a capacitance which must be added to the circuit model of a p–n diode. The junction capacitance dominates for the reverse-biased diodes, while the diffusion capacitance dominates in strongly forward-biased diodes [44]. Fig. 7 illustrates the variation of the junction capacitance with the bias voltage at frequency of 500 kHz for the Al/OG/p-Si MIS device. In addition, Fig. 7 shows C^{-2}–V characteristic of the Al/OG/p-Si MIS device. The C^{-2}–V plot is linear which indicates the formation of Schottky junction [45]. By using standard Mott–Schottky relationship between capacitance–voltage [16,17], the values of diffusion potential (V_d), barrier height and acceptor carrier concentration (N_A) for the Al/OG/p-Si MIS device were extracted as 0.91 V, 1.17 eV and 4.94×10^{14} cm^{-3} from the linear region of its C^{-2}–V characteristic, respectively. As seen from the obtained values, the difference between Φ_b(I–V) and Φ_b(C–V) for the Al/OG/p-Si MIS diode originates from the different nature of the I–V and C–V measurements. Due to different nature of the C–V and I–V measure-

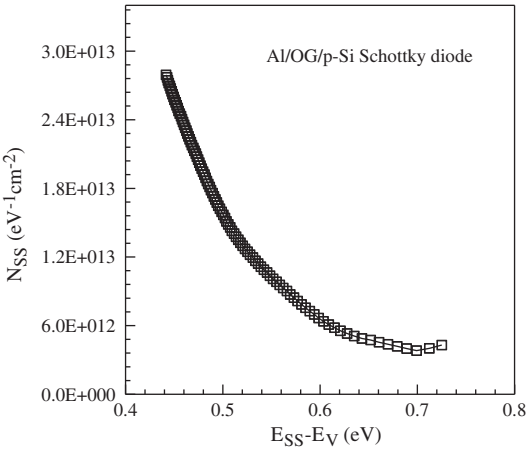

Fig. 6. N_{SS} – (E_{SS}–E_V) plot of the Al/OG/p-Si MIS device.

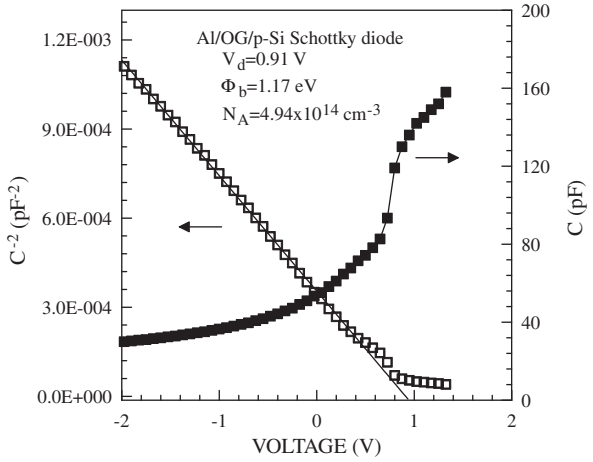

Fig. 7. C–V and C^{-2}–V characteristics of the Al/OG/p-Si MIS diode.

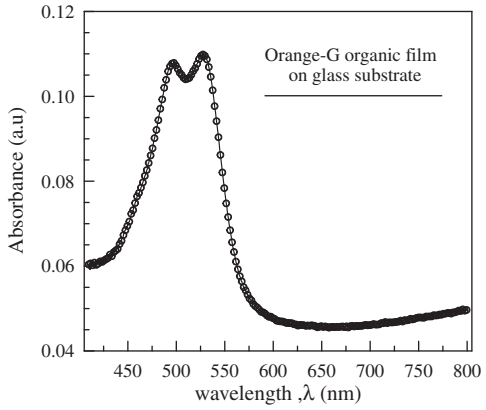

Fig. 8. Optical absorbance spectrum of the OG organic film on a glass substrate.

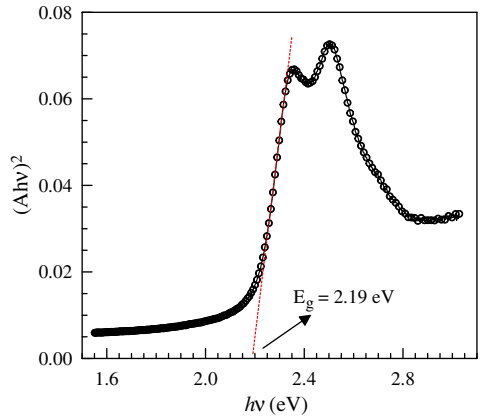

Fig. 9. The plot of $(Ahv)^2$ vs. hv of the OG organic film on a glass substrate.

ment techniques, barrier heights deduced from them are not always the same. The capacitance C is insensitive to potential fluctuations on a length scale of less than the space charge region and C–V method averages over the whole area and measures to describe BH. The DC current I across the interface depends exponentially on barrier height and thus sensitively on the detailed distribution at the interface [16,46]. Additionally, the discrepancy between the barrier height values of the devices may also be explained by the existence of an interfacial layer and trap states in semiconductor [38,47].

3.4. Optical properties of OG organic thin film

Optical absorbance spectrum of the OG organic film on a glass substrate was analyzed by the following relationship:

$$Ahv = B(hv - E_g)^m, \tag{10}$$

where B is a constant, E_g is the optical band gap, A is absorbance of the film. The exponent m depends on the nature of the transition, $m = 1/2$, 2, 3/2, or 3 for allowed direct, allowed non-direct, forbidden direct or forbidden non-direct transitions, respectively. Fig. 8 shows optical absorbance spectrum of the OG organic film on the glass substrate. The distinctly characterized peaks in the visible region are generally been interpreted in terms of π–π^* excitation between bonding and antibonding molecular orbitals [48]. Fig. 9 shows the plot of $(Ahv)^2$ vs. hv according to Eq. (10). Satisfactory fit is obtained for $(Ahv)^2$ vs. hv indicating the presence of a direct band gap [48,49]. The optical energy gap E_g of the organic film was determined as 2.19 eV by extrapolating the linear portion of this plot at $(Ahv)^2 = 0$ which indicates that the direct allowed transition dominates in the OG film.

4. Conclusion

In summary, we have investigated the electrical characteristics of the Al/OG/p-Si MIS Schottky structures formed by coating of the organic material to directly p-Si substrate. It has been seen that the OG thin film on p-Si substrate showed a good rectifying behavior. The barrier height and the ideality factor of the device were calculated from the I–V characteristic. We have also studied the suitability and possibility of organic-on inorganic semiconductor diodes for using in the barrier modification of Si MS diodes. In addition, we have compared the parameters of the Al/OG/p-Si MIS Schottky diodes with those of conventional MS diodes. We have observed that the Φ_b value of 0.77 eV obtained for the Al/OG/p-Si device was significantly larger than the BH value of the conventional Al/p-Si MS contact. Thus, the modification of the interfacial potential barrier for metal/Si diodes has been achieved by using an OG organic interlayer. This has been attributed to the fact that the OG interlayer increased the effective Φ_b by influencing the space charge region of Si. The interface-state density of the MIS diode was found to vary from 2.79×10^{13} to 5.80×10^{12} eV^{-1} cm^{-2}.

Acknowledgements

The authors wish to thank Dr. O. Baris (Atatürk University) and Dr. M. Cankaya (Erzincan University) for the organic material supply. The English text has been kindly checked by Lecturer Mr. Ihsan Pilatin from Batman University.

References

[1] A. Al-Mohamad, C.W. Smith, I.S. Al-Saffar, M.A. Slifkin, Thin Solid Films 189 (1) (1990) 175.
[2] G.D. Sharma, S.K. Sharma, M.S. Roy, Thin Solid Films 468 (1–2) (2004) 208.
[3] T.S. Shafai, Thin Solid Films 517 (3) (2008) 1200.
[4] M.S. Roy, G.D. Sharma, S.K. Gupta, Thin Solid Films 310 (1–2) (1997) 279.
[5] M.E. Aydin, F. Yakuphanoglu, T. Kılıçoğlu, Synth. Met. 157 (24) (2007) 1080.
[6] K.R. Rajesh, C.S. Menon, J. Non-Cryst. Solids 353 (4) (2007) 398.
[7] T. Kilicoglu, M.E. Aydin, Y.S. Ocak, Physica B 388 (1–2) (2007) 244.
[8] S.R. Forrest, M.L. Kaplan, P.H. Schmidt, W.L. Feldmann, E. Yanowski, Appl. Phys. Lett. 41 (1982) 90.
[9] R.K. Gupta, R.A. Singh, Mater. Chem. Phys. 86 (2004) 279.
[10] M.E. Aydin, T. Kilicoglu, K. Akkilic, H. Hosgoren, Physica B 381 (2006) 113.
[11] S.R. Forrest, M.L. Kaplan, P.H. Schmidt, J. Appl. Phys. 55 (1984) 1492.
[12] S. Antohe, N. Tomozeiu, S. Gogonea, Phys. Status Solidi A 125 (1991) 397.
[13] M.A. Ebeoglu, T. Kilicoglu, M.E. Aydin, Physica B 395 (2007) 93.
[14] S.A. Moiz, M.M. Ahmed, K.S. Karimov, ETRI J. 27 (3) (2005) 319.
[15] O. Gullu, O. Baris, M. Biber, A. Turut, Appl. Surf. Sci. 254 (2008) 3039.
[16] E.H. Rhoderick, R.H. Williams, Metal–Semiconductor Contacts, second ed., Oxford, Clarendon, 1988.
[17] S.M. Sze, Physics of Semiconductor Devices, second ed., Wiley, New York, 1981.
[18] R.F. Schmitsdorf, T.U. Kampen, W. Monch, J. Vac. Sci. Technol., B 15 (4) (1997) 1221.
[19] W. Monch, J. Vac. Sci. Technol., B 17 (4) (1999) 1867.
[20] R.T. Tung, Phys. Rev. B 45 (23) (1992) 13509.
[21] G.M. Vanalme, L. Goubert, R.L. Van Meirhaeghe, F. Cardon, P. Van Daele, Semicond. Sci. Technol. 14 (1999) 871.
[22] Y.S. Lou, IEEE Trans. Electron Devices 41 (4) (1994) 558.
[23] F. Yakuphanoglu, M. Kandaz, B.F. Senkal, Thin Solid Films 516 (2008) 8793.
[24] C. Temirci, M. Çakar, Physica B 348 (2004) 454.
[25] Ş. Karatas, C. Temirci, M. Çakar, A. Türüt, Appl. Surf. Sci. 252 (2006) 2209.
[26] M. Çakar, C. Temirci, A. Türüt, Synth. Met. 142 (2004) 177.
[27] M. Çakar, Y. Onganer, A. Türüt, Synth. Met. 126 (2002) 213.
[28] T. Kampen, A. Schuller, D.R.T. Zahn, B. Biel, J. Ortega, R. Perez, F. Flores, Appl. Surf. Sci. 234 (2004) 341.
[29] A.R.V. Roberts, D.A. Evans, Appl. Phys. Lett. 86 (2005) 072105.
[30] A. Bolognesi, A. DiCarlo, P. Lugli, T. Kampen, D.R.T. Zahn, J. Phys.: Condens. Matter 15 (2003) S2719.
[31] D.R.T. Zahn, T.U. Kampen, H. Mendez, Appl. Surf. Sci. 212 (2003) 423.
[32] S. Aydogan, M. Saglam, A. Turut, Microelectron. Eng. 85 (2008) 278.
[33] A. Turut, M. Saglam, H. Efeoglu, N. Yalcin, M. Yildirim, B. Abay, Physica B 205 (1995) 41.

[34] S.K. Cheung, N.W. Cheung, Appl. Phys. Lett. 49 (1986) 85.
[35] T. Kilicoglu, Thin Solid Films 516 (2008) 967.
[36] S. Karatas, S. Altindal, A. Turut, M. Cakar, Physica B 392 (1–2) (2007) 43.
[37] O. Gullu, S. Aydogan, A. Turut, Microelectron. Eng. 85 (2008) 1647.
[38] H.C. Card, E.H. Rhoderick, J. Phys. D 4 (1971) 1589.
[39] M. Çakar, N. Yıldırım, H. Doğan, A. Türüt, Appl. Surf. Sci. 253 (2007) 3464.
[40] M.E. Aydin, A. Türüt, Microelectron. Eng. 84 (2007) 2875.
[41] T.U. Kampen, S. Park, D.R.T. Zahn, Appl. Surf. Sci. 190 (2002) 461.
[42] M. Cakar, N. Yildirim, S. Karatas, C. Temirci, A. Turut, J. Appl. Phys. 100 (2006) 074505.
[43] S.R. Forrest, M.L. Kaplan, P.H. Schmidt, J. Appl. Phys. 60 (1986) 2406.
[44] C.H. Chen, I. Shih, J. Mater. Sci: Mater. Electron. 17 (2006) 1047.
[45] V. Saxena, K.S.V. Santhanam, Curr. Appl. Phys. 3 (2003) 227.
[46] J.H. Werner, H.H. Guttler, J. Appl. Phys. 69 (1991) 1522.
[47] O. Gullu, M. Cankaya, M. Biber, A. Turut, J. Phys.: Condens. Matter 20 (2008) 215210.
[48] K.R. Rajesha, C.S. Menon, Eur. Phys. J. B 47 (2005) 171.
[49] O. Gullu, A. Turut, Sol. Energy Mater. Sol. Cells 92 (10) (2008) 1205.